

Epitaxial BiFeO₃ thin films on Si

Cite as: Appl. Phys. Lett. **85**, 2574 (2004); <https://doi.org/10.1063/1.1799234>

Submitted: 19 April 2004 . Accepted: 30 July 2004 . Published Online: 28 September 2004

J. Wang, H. Zheng, Z. Ma, S. Prasertchoung, M. Wuttig, R. Droopad, J. Yu, K. Eisenbeiser, and R. Ramesh



View Online



Export Citation

ARTICLES YOU MAY BE INTERESTED IN

[Dramatically enhanced polarization in \(001\), \(101\), and \(111\) BiFeO₃ thin films due to epitaxial-induced transitions](#)

Applied Physics Letters **84**, 5261 (2004); <https://doi.org/10.1063/1.1764944>

[Leakage mechanisms in BiFeO₃ thin films](#)

Applied Physics Letters **90**, 072902 (2007); <https://doi.org/10.1063/1.2535663>

[Photovoltaic effects in BiFeO₃](#)

Applied Physics Letters **95**, 062909 (2009); <https://doi.org/10.1063/1.3204695>



New

Your Qubits. Measured.

Meet the next generation of quantum analyzers

- Readout for up to 64 qubits
- Operation at up to 8.5 GHz, mixer-calibration-free
- Signal optimization with minimal latency

Find out more



Epitaxial BiFeO₃ thin films on Si

J. Wang,^{a)} H. Zheng, Z. Ma, S. Prasertchoung, and M. Wuttig
Department of Materials Science and Engineering, University of Maryland, College Park, Maryland 20742

R. Droopad, J. Yu, and K. Eisenbeiser
Motorola Phoenix Research Laboratories, Tempe, Arizona 85284

R. Ramesh
Department of Materials Science and Engineering and Department of Physics, University of California, Berkeley, California 94720

(Received 19 April 2004; accepted 30 July 2004)

BiFeO₃ was studied as an alternative environmentally clean ferro/piezoelectric material. 200-nm-thick BiFeO₃ films were grown on Si substrates with SrTiO₃ as a template layer and SrRuO₃ as bottom electrode. X-ray and transmission electron microscopy studies confirmed the epitaxial growth of the films. The spontaneous polarization of the films was $\sim 45 \mu\text{C}/\text{cm}^2$. Retention measurement up to several days showed no decay of polarization. A piezoelectric coefficient (d_{33}) of $\sim 60 \text{ pm}/\text{V}$ was observed, which is promising for applications in micro-electro-mechanical systems and actuators. © 2004 American Institute of Physics.
 [DOI: 10.1063/1.1799234]

Perovskite BiFeO₃ (BFO) has attracted much attention recently due to the coexistence of ferroelectric and magnetic orders. It has high Curie ($T_C \sim 1100 \text{ K}$) and Neel ($T_N \sim 673 \text{ K}$) temperatures. In the bulk, it possesses a rhombohedrally distorted perovskite structure with space group $R3c-C_{3v}^6$.¹ The rhombohedral and pseudocubic unit cell parameters are $a = 5.616(6) \text{ \AA}$, $\alpha = 59.35(5)^\circ$,² and $a = 3.96 \text{ \AA}$, respectively. Electrical characterization of bulk single crystal samples has been difficult due to their very low resistivity. Teague *et al.* reported a polarization of $3.5 \mu\text{C}/\text{cm}^2$ along (001) at 70 K, indicating a polarization of $6.1 \mu\text{C}/\text{cm}^2$ along (111),³ which is much smaller than expected from a material with such a high Curie temperature and large distortion. Recently, it has been reported that both epitaxial and polycrystalline BFO thin films with reasonably high resistivity show large polarizations.^{4,5} For example, (001) oriented thin films BFO display a polarization of $\sim 55 \mu\text{C}/\text{cm}^2$, comparable to the very popular ferroelectric system, $\text{Pb}(\text{Zr}_x\text{Ti}_{1-x})\text{O}_3$ (PZT), which has been studied for decades for applications in memory, transducers, and micro-electro-mechanical system (MEMS). An aspect of concern with the PZT system is its relative toxicity accruing from lead. BFO provides an alternative choice of a Pb-free ferro/piezoelectric material, which is environmentally preferable. Approaches to grow high quality BFO films on Si substrates are desirable. Such an approach is demonstrated in this letter using a template layer consisting of epitaxial SrTiO₃ (STO) deposited directly on Si by molecular-beam epitaxy,^{6,7} which was previously used for the integration of PZT with Si.^{8,9}

200 nm BFO thin films were grown by pulsed laser deposition. To ensure heteroepitaxial growth, 20 nm SrRuO₃ (SRO) was chosen as bottom electrode. Details of deposition parameters are listed in Table I. After deposition, the films were annealed at 390 °C for 1 h during cooling (5 °C/min) in 1 atm oxygen ambient. X-ray diffraction (Siemens D5000 four-circle diffractometer) and transmission electron micros-

copy [(TEM), JEOL 4000FX operating at 300 kV] were used to characterize the film structure. Ferroelectric property measurements were performed with a commercially available RT6000 test system (Radiant Technologies, USA). Piezoelectric measurements were done using a setup based on an atomic force microscope,⁴ while the dielectric constant was determined by a HP impedance analyzer.

A typical x-ray $\theta-2\theta$ scan, Fig. 1(a), shows only (00l) diffraction peaks from BFO and SRO in addition to Si peaks (not shown). No reflections were detected that would be indicative of second phases. A phi scan of the BFO (202) and Si (404) planes is displayed as inset of Fig. 1(a). Only four sharp peaks originate from BFO indicating that the film has good in-plane orientation. The inset also reveals a 45° rotation of BFO with respect to the Si substrate. Selected area electron diffraction from a cross-section TEM sample, Fig. 1(b), confirmed this rotation. The diffraction patterns originating from SRO, STO overlap with that from BFO, indicating that both SRO and BFO grow cubic-on-cubic with respect to STO. These results can be understood on the basis of the lattice match $d_{\text{SRO}(100)} = 3.94 \text{ \AA}$, $d_{\text{STO}(100)} = 3.91 \text{ \AA}$ with $d_{\text{Si}(110)} = 3.82 \text{ \AA}$. The out-of-plane lattice constant of BFO was calculated to be $\sim 3.95 \text{ \AA}$ (pseudocubic unit), which is smaller than its bulk value. The film is likely to have monoclinic structure. This observation is a consequence of two competing effects: (a) the compressive stress imposed by the SRO/STO layers, which have in-plane lattice parameters smaller than that of BFO; and (b) a tensile stress due to the thermal mismatch of Si and the oxides (Si: $\alpha \sim 3 \times 10^{-6} \text{ deg}^{-1}$, BFO: $\alpha \sim 1 \times 10^{-5} \text{ deg}^{-1}$). Since the films

TABLE I. Summary of deposition parameters used for SRO and BFO films.

| Film | Substrate temperature (°C) | Energy density (J/cm ²) | O ₂ partial pressure (m Torr) | Deposition rate (nm/min) |
|------|----------------------------|-------------------------------------|--|--------------------------|
| SRO | 650 | ~ 1.2 | 100 | ~ 0.7 |
| BFO | 670 | ~ 1.2 | 40 | ~ 7 |

^{a)}Electronic mail: jlwang@wam.umd.edu

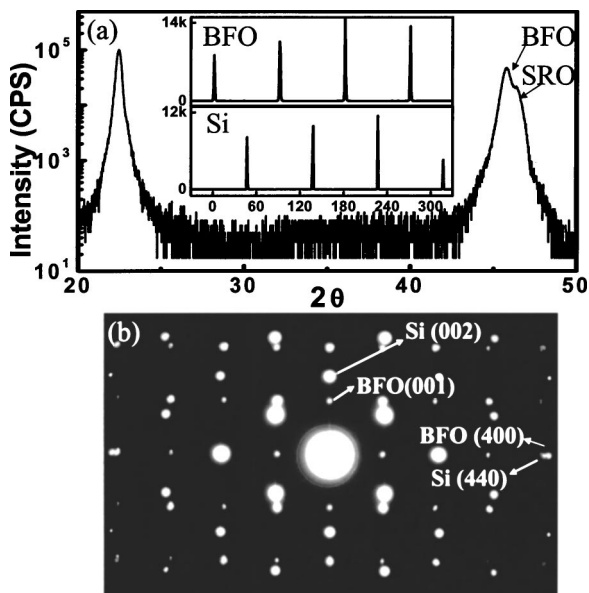


FIG. 1. (a) Typical $\theta-2\theta$ scan of a BiFeO₃/SrRuO₃/SrTiO₃/Si sample. No second phase was observed. ψ scans of BiFeO₃ (202) and Si (404) indicate a 45° rotation of BiFeO₃ unit with respect to Si. (b) Electron diffraction pattern confirms the epitaxial growth the films.

are thicker than the expected critical thickness for dislocation formation, we expect that the thermal stress dominates at room temperature, leading to an in-plane tensile stress and the decrease in the out-of-plane lattice parameter.

Ferroelectric properties were characterized using both polarization hysteresis as well as pulsed polarization measurements. We use Pt as top electrode. Figure 2(a) shows a set of hysteresis loops measured on a 32- μ m-diam capacitor at a frequency of 15 kHz. A remnant polarization of $P_r \sim 45 \mu\text{C}/\text{cm}^2$ is observed, which is smaller than that of films grown on single crystal STO substrates ($\sim 55 \mu\text{C}/\text{cm}^2$ on [100] STO and $\sim 95 \mu\text{C}/\text{cm}^2$ on [111] STO).¹¹ This can be understood as a consequence of the smaller c/a ratio of BFO on Si. Pulse polarization measurements that are less likely convoluted by leakage and nonlinear dielectric effects, confirmed this result. Figure 2(b) shows the pulsed remnant polarization, ($\Delta P = P^* - P^\wedge \approx 2P_r$, where P^* is the switched polarization and P^\wedge is the nonswitched polarization) versus applied electric field, measured using 10 μ s pulses. We ob-

served an increase of ΔP around 3 V reaching a value of $\sim 100 \mu\text{C}/\text{cm}^2$ at 12 V. For use in memory applications, the coercive field (which is currently $\sim 2-3$ V for 200 nm film) has to be lowered to about 0.7–1 V. In the case of PZT thin films, this has been shown to be possible through cationic substitutions, which tunes the tetragonality of the material. Our preliminary experiments using La substitution at the Bi site suggest a similar prospect in the BFO system. The films display resistivity values of $\sim 10^9 \Omega \text{ cm}$ at zero bias, lower than those of typical perovskite ferroelectric oxides like PZT, and possibly due to defects, i.e., oxygen vacancies. The pulse width dependence of ΔP down to 1 μ s is shown in Fig. 2(c). The stability of the polar state is confirmed by retention measurements as shown in Fig. 2(d). No significant change of the polarization was observed over a period of several days.

Piezoelectric hysteresis loop, Fig. 3(a), shows a remnant d_{33} value of 60 pm/V for the fully clamped film, which is comparable to that obtained from Ti-rich PZT films (Zr/Ti ratio of 20/80). Figure 3(b) shows the small signal dielectric constant, ϵ_r , for a 32 μ m capacitor. The observed ϵ_r was ~ 170 .

We have also studied the thickness dependence of the polarization, piezoelectric coefficient, and dielectric constant of the epitaxial BFO films on Si. Figure 4 contains the summary of the results. The out-of-plane lattice constant decreases as the film thickness increases from 100 to 400 nm, which can be understood by considering the relaxation of the compressive stress originating from SRO/STO layers, while keeping in mind that the dominating thermal mismatch reduces the bulk value of the out-of-plane lattice constant. Figure 4 also shows the switchable polarization, ΔP , measured at constant electric field (400 kV/cm, corresponding to 8 V for 200 nm film). The change in ΔP is relatively small. On the other hand, the piezoelectric constant d_{33} shows a dramatic increase from ~ 30 pm/V for a 100 nm film to ~ 120 pm/V for a 400 nm film; the dielectric constant follows the same trend as d_{33} . We have observed similar behavior in the BFO films grown on STO substrates.⁴

In summary, epitaxial BFO thin films were grown on Si substrate using a STO template layer. A significant polarization, $\sim 45 \mu\text{C}/\text{cm}^2$, was observed at room temperature for a 200 nm film. Retention analyses up to several days confirmed the polarization stability. 400-nm-thick films possess

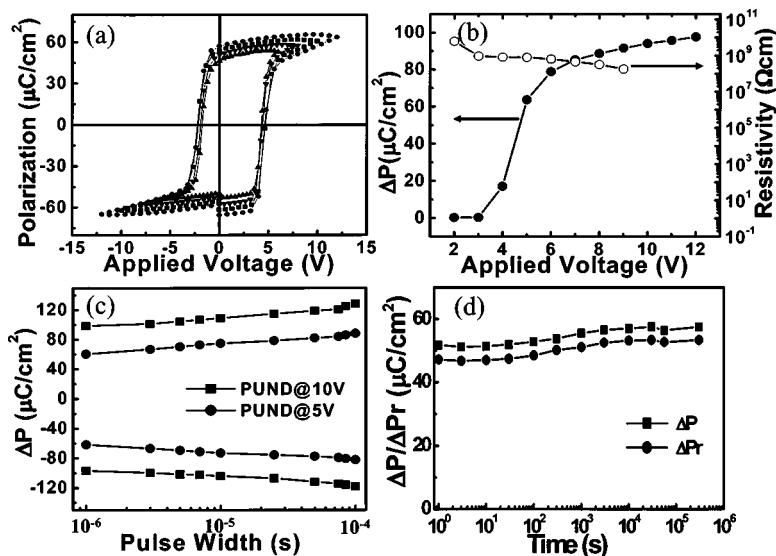


FIG. 2. (a) Ferroelectric hysteresis measured at a frequency of 15 kHz. The remnant polarization equals $\sim 45 \mu\text{C}/\text{cm}^2$. (b) Pulsed polarization, ΔP vs electric field, determined with electrical pulses of 10 μ s width and resistivity vs electric field measured using 1 s pulses. (c) Pulse width dependence of ΔP . (d) Polarization retention showing no significant change after several days.

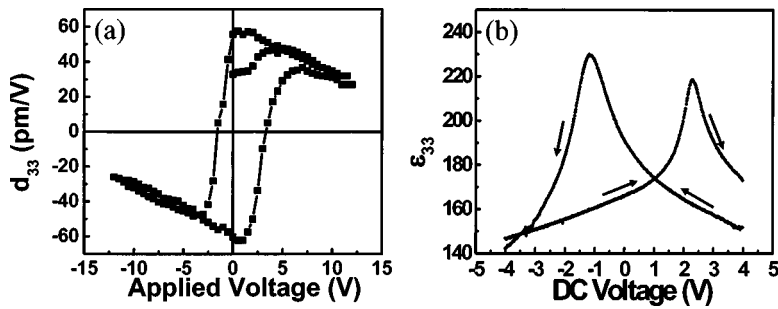


FIG. 3. (a) Small signal d_{33} , (b) Small signal dielectric constant, ϵ_r , of a $32 \mu\text{m}$ capacitor.

a large piezoelectric coefficient, $\sim 120 \text{ pm/V}$, which is useful for applications in MEMS and actuators.

This work is supported by the Office of Naval Research (Grant No. MURI N000140110761) and the NSF-MRSEC (Grant No. MRSEC DMR-00-80008). It also benefits from the support of NSF Grant No. DMR0095166. The NSF-MRSEC has provided support for the pulsed laser deposition system used in this research.

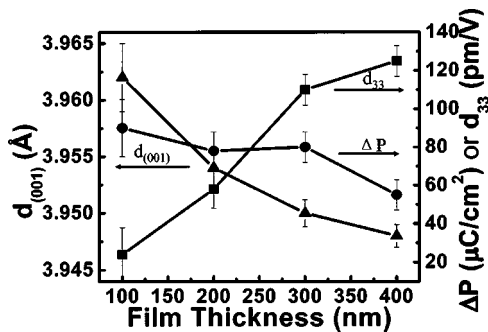


FIG. 4. Thickness dependence of the out-of-plane lattice constant, polarization, and piezoelectric coefficient.

¹C. Michel, J.-M. Moreau, G. D. Achenbach, R. Gerson, and W. J. James, *Solid State Commun.* **7**, 701 (1969).

²J. J. Jacobson and B. F. F. Fender, *J. Phys. C* **8**, 844 (1975).

³J. R. Teague, R. Gerson, and W. J. James, *Solid State Commun.* **8**, 1073 (1970).

⁴J. Wang, J. B. Neaton, H. Zheng, V. Nagarajan, S. B. Ogale, B. Liu, D. Viehland, V. Vaithyanathan, D. G. Schlom, U. V. Waghmare, N. A. Spaldin, K. M. Rabe, M. Wuttig, and R. Ramesh, *Science* **299**, 1719 (2003).

⁵K. Y. Kun, M. Noda, and M. Okuyama, *Appl. Phys. Lett.* **83**, 3981 (2003).

⁶K. Eisenbeiser, J. M. Finder, Z. Yu, J. Ramdani, J. A. Curless, J. A. Hallmark, R. Droopad, W. J. Ooms, L. Salem, S. Bradshaw, and C. D. Overgaard, *Appl. Phys. Lett.* **76**, 1324 (2000).

⁷R. A. McKee, F. J. Walker, and M. F. Chisholm, *Phys. Rev. Lett.* **81**, 3014 (1998).

⁸Y. Wang, C. Ganpule, B. T. Liu, H. Li, K. Mori, B. Hill, M. Wuttig, R. Ramesha, J. Finder, Z. Yu, R. Droopad, and K. Eisenbeiser, *Appl. Phys. Lett.* **80**, 97 (2002).

⁹B. T. Liu, K. Maki, Y. So, V. Nagarajan, R. Ramesha, J. Lettieri, J. H. Haeni, D. G. Schlom, W. Tian, X. Q. Pan, F. J. Walker, and R. A. McKee, *Appl. Phys. Lett.* **80**, 4801 (2002).

¹⁰J. D. Bucci, B. K. Robertson, and W. J. James, *J. Appl. Crystallogr.* **5**, 187 (1972).

¹¹J. F. Li, J. Wang, M. Wuttig, R. Ramesh, N. Wang, B. Ruetter, A. P. Pyatakov, A. K. Zvezdin, and D. Viehland, *Appl. Phys. Lett.* **84**, 5261 (2004).